

Optical confirmation of the extended mean-field theory for a smectic- C^* –smectic- A transition

Fuzi Yang, G. W. Bradberry, and J. R. Sambles

Thin Film and Interface Group, Department of Physics, University of Exeter, Stocker Road, Exeter EX4 4QL, United Kingdom

(Received 31 May 1994)

Half-leaky guided modes are used to determine accurately the cone angle in a smectic- C^* liquid crystal as a function of temperature. Homeotropic alignment is obtained using only an in-plane electric field and electroclinic and voltage-induced effects are made negligible. The data obtained is fitted fully to an extended mean-field theory using the cone angle as a measure of the order parameter. The results show unequivocally for this material, the ferroelectric liquid crystal SCE13, that the free energy is fully specified through an expression containing terms to third order in the cone angle squared.

PACS number(s): 64.70.Md, 61.30.Eb

INTRODUCTION

A model proposed by deGennes [1] suggests that the second order S_A to S_C phase transition behaves in a similar manner to the critical behavior observed in superfluid helium, that is the transition should be in the $d=3, n=2$ universality class (a three dimensional XY model). Following this proposal, experiments on the tilt angle (cone angle, θ) lead to critical exponents which varied from criticallike [2–4] to mean-field-like [5] while heat capacity measurements [6,7] indicated a mean-field behavior. In an endeavor to fully explain their heat capacity measurements Huang and Viner [7] developed an extended mean-field theory by introducing a third-order term (in the tilt angle squared) into the Landau free-energy expansion. The significance of this term has been confirmed by further high-resolution heat capacity measurements on a range of materials [8–12].

Huang and co-workers [13–15] later extended their measurements to the smectic- A –chiral smectic- C^* (S_C^*) transition. For this transition there are various extra coupling terms involving the polarization, P , or the helical pitch wave vector, q , which are needed to describe the S_C^* phase in terms of the free-energy expansion. However, they found that the extra terms involving P and q are sufficiently small such that the extended mean-field theory is still an excellent description of the heat capacity and tilt angle data in the vicinity of the S_A - S_C^* transition.

Their data reveal an unusually strong third-order (in tilt angle squared) term which results in the crossover temperature, separating the ordinary mean-field region from the tricritical region, being very close to the phase transition temperature T_C . Consequently, a power law fitting of the tilt angle as a function of temperature leads to a critical exponent ranging from 0.25 to 0.5. These are inevitably misleading numbers, the answer depending on the temperature range over which data is recorded.

More direct measurements of tilt angles using optical probes are strongly influenced by the strength of surface anchoring, the quality of director alignment and the thickness of the cell. Thus determination of the order pa-

rameter through establishing the tilt angle has been problematic and heat capacity measurements have dominated. However, if the alignment difficulties can be overcome then optical determination of the tilt angle should provide an excellent test of the models describing the S_C - S_A phase transition. It is just such a test which is reported here.

EXPERIMENT

A homeotropically aligned cell is produced with no surface aligning layer. Instead monodomain homeotropic alignment is established by applying a field in the plane of the liquid crystal filled cell with the material (Merck, SCE13) held at a temperature close to the S_A - S_C^* phase transition temperature. With an electric field applied (>1000 V applied between electrodes spaced 3 mm apart) the helix is unwound and the sample forms a monodomain with the primary director approximately at the tilt angle to the cell surface and tilted in a plane orthogonal to the electric field. The sample geometry is illustrated in Fig. 1.

Use of a high-index prism and a low-index glass substrate (with no surface coatings to ensure very weak surface forces) separated by $3.5 \mu\text{m}$ mylar spacers provides

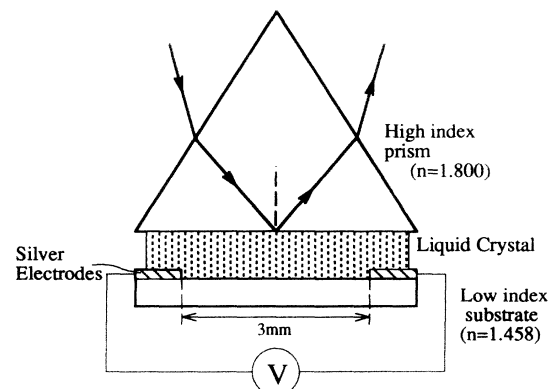


FIG. 1. The experimental geometry for the tilt angle measurements.

the requisite half-leaky guided mode geometry [16] for detailed optical characterization of the director profile. The two silver electrodes are evaporated onto the low-index substrate with a gap of 3 mm to allow the application of the in-plane electric field. This empty cell is placed in a thermal environment, stabilized to $\pm 0.02^\circ\text{C}$, and heated to 110°C . It is then capillary filled with SCE13 and quickly cooled to about 62°C in the S_A phase. Then with 1.5 kV dc applied between the electrodes it is cooled at a rate of less than 0.5°C per hour to about 52°C , well into the S_C^* phase. Finally, cooling to 24.1°C is completed over a period of a few hours. Subsequently data is recorded, at chosen temperatures and under specific applied potentials, in the form of s (transverse electric) to p (transverse magnetic) conversion reflectivity

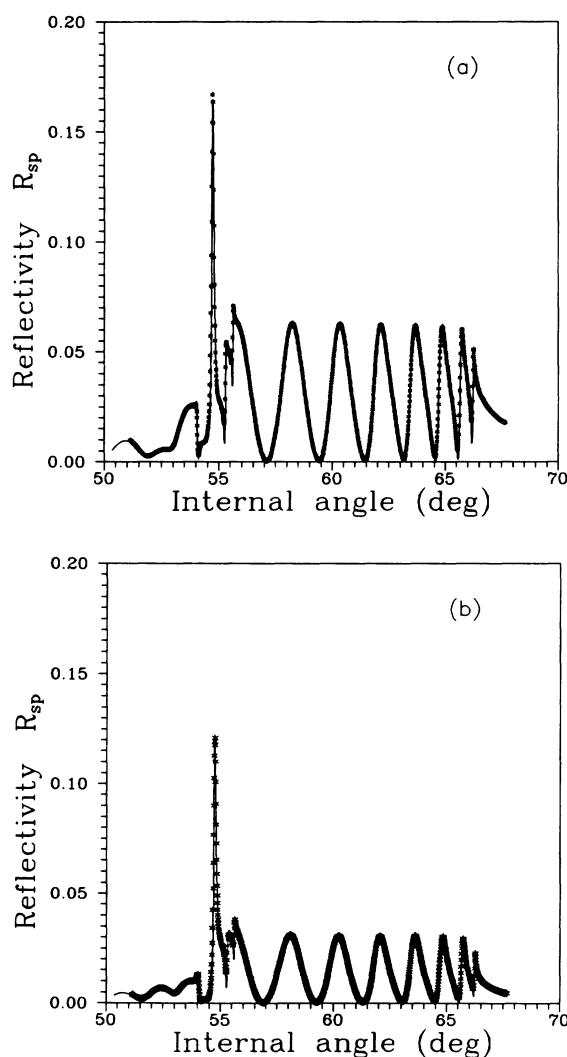


FIG. 2. Experimental (crosses) and theoretical (solid line) s to p conversion reflectivity data, R_{sp} , for a wavelength of 632.8 nm. (a) and (b) show the effect of applying the dc electric field in opposite directions. The fitted parameters are $\epsilon_1(\text{prism})=3.2400$; liquid crystal $\epsilon_{\parallel}=2.7210+i0.0003$, $\epsilon_{\perp}=2.2115+i0.0003$; thickness = $3.76 \mu\text{m}$, $\epsilon_3=2.126$. The fitted tilt angles are 9.10° and 6.80° for (a) and (b), respectively.

against angle of incidence. The laser beam (wavelength of 632.8 nm) is incident midway between the two electrodes to ensure no anchoring forces from the electrode edges. Illustrative sets of experimental data taken at 53.57°C (crosses) compared with theoretical predictions (solid line) are shown in Fig. 2. These two data sets taken with $+1.5$ and -1.5 kV applied, respectively, show very clearly that the S_C^* density wave normal is at an angle to the cell plane. If this were not so then the signals should be identical and the tilt angles, γ_+ , γ_- , would be just $+\theta$ and $-\theta$, respectively. However, with a density wave tilt δ then one total tilt angle is $\gamma_+ (= \theta + \delta)$, the other $\gamma_- (= -\theta + \delta)$, and hence the two polarization convergent signals are different in magnitude. For these two sets fitting with a model which comprises primarily a uniformly tilted slab, but with very thin surface regions (< 20 nm) over which the tilt is assumed to vary linearly from the bulk tilt to the surface normal, results in $\epsilon_{\parallel}=2.7210+i0.0003$ and $\epsilon_{\perp}=2.2115+i0.0003$ with a tilt of 9.10° for the data in Fig. 2(a) and 6.80° for data in Fig. 2(b). This leads to a density wave tilt of 1.15° and a tilt, or cone, angle of 7.95° (as illustrated in Fig. 3). Note that while from homogeneously aligned cells there is evidence for optical biaxiality, in the homeotropic alignment used here this will have a negligible effect.

The fact that an almost entirely uniform tilted slab gives such superb fits to the data shows that unwinding of the S_C^* helix is completed at 1.5 kV. In fact, reducing the voltage to 800 V results in no significant change suggesting this lower voltage, equivalent to an electric field of $0.3 \text{ V}\mu\text{m}^{-1}$ is sufficient to fully unwind the helix. Thus, from this very simple geometry we were able to determine a wealth of useful information on the behavior of

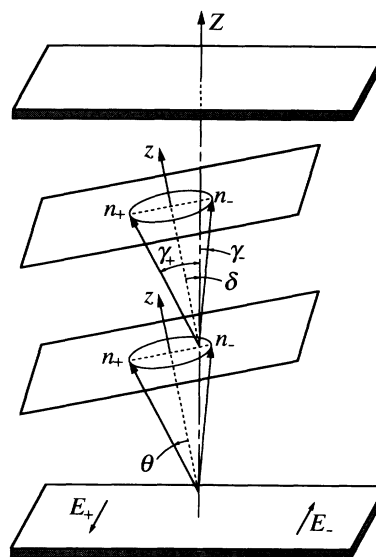


FIG. 3. The geometry associated with the unwinding of the helix with an applied dc electric field. θ is the cone angle of the liquid crystal and δ the angle between the normal to the cell wall and the normal of the layers. n_+ , γ_1 and n_- , γ_2 are the unwound primary directors and measured tilt angle under positive E_+ and negative E_- dc fields, respectively.

the liquid crystal.

Let us now concentrate only on the measurement of the tilt angle. If one is to compare such measurements to theory then we have to be certain that the results are effectively zero field results to avoid the influence of electroclinic effects. Increasing the field should cause a progressive increase in tilt angle. In order to establish the magnitude of this effect at any given temperature data for at least five different voltages were taken and the tilt angle extrapolated back to the zero field limit. In fact, it is only very near the phase transition temperature that a voltage as large as 1.5 kV changes the tilt by more than 2.0° . So it is really very simple to obtain highly accurate cone angle data.

However, since the electroclinic effect is strongest near the phase transition it is apparent that determining this phase transition temperature could be difficult. Yet, this is a fundamental measurement which must be known accurately if we are to reliably compare phase transition theory with data. Consider what happens as the applied voltage of +1.5 kV is slowly reduced to zero—the helix will start to unwind from the positive orientation and at zero volts we will record a signal from a partially wound helix with the wave vector normal tilt of order 1.15° and some cone angle. Then applying -1.5 kV and reducing the voltage to zero once again a different signal at zero volts will be recorded since the helix is now unwound from the negative orientation with again a wave vector normal tilt of order 1.15° and some cone angle. If, however, we are at or above the phase transition the cone angle will be zero and the two zero voltage traces will be indistinguishable. Three pairs of zero volt traces obtained in this manner are shown in Fig. 4. Just 0.2° below the phase transition the two traces are very different. As the temperature increases towards the phase transition the traces became similar and eventually identical at the transition temperature. Careful use of this procedure allows the determination of the phase transition temperature as $55.81 \pm 0.02^\circ\text{C}$.

So now we may establish the final data set of tilt angle (measured to $\pm 0.05^\circ$) against the temperature difference between the phase transition temperature, T_c , and the measurement temperature, T . All the data for the full temperature range is presented in Fig. 5. The solid line is the best polynomial fit to the equation:

$$(T_c - T) = A\theta^2 + B\theta^4, \quad (1)$$

with $A = 95$ and $B = 500$.

In the extended mean-field model proposed by Huang and Viner [7] the free energy is given as

$$G = G_0 + at\theta^2 + b\theta^4 + c\theta^6, \quad (2)$$

where G_0 is the nonsingular part of the free energy and $t = (T - T_c)/T_c$ is the reduced temperature. T_c being the phase transition temperature in Kelvin. The coefficients a , b , and c are greater than zero for a continuous second-order transition.

Minimizing G with respect to θ gives

$$a(T_c - T) = 2bT_c\theta^2 + 3cT_c\theta^4, \quad (3)$$

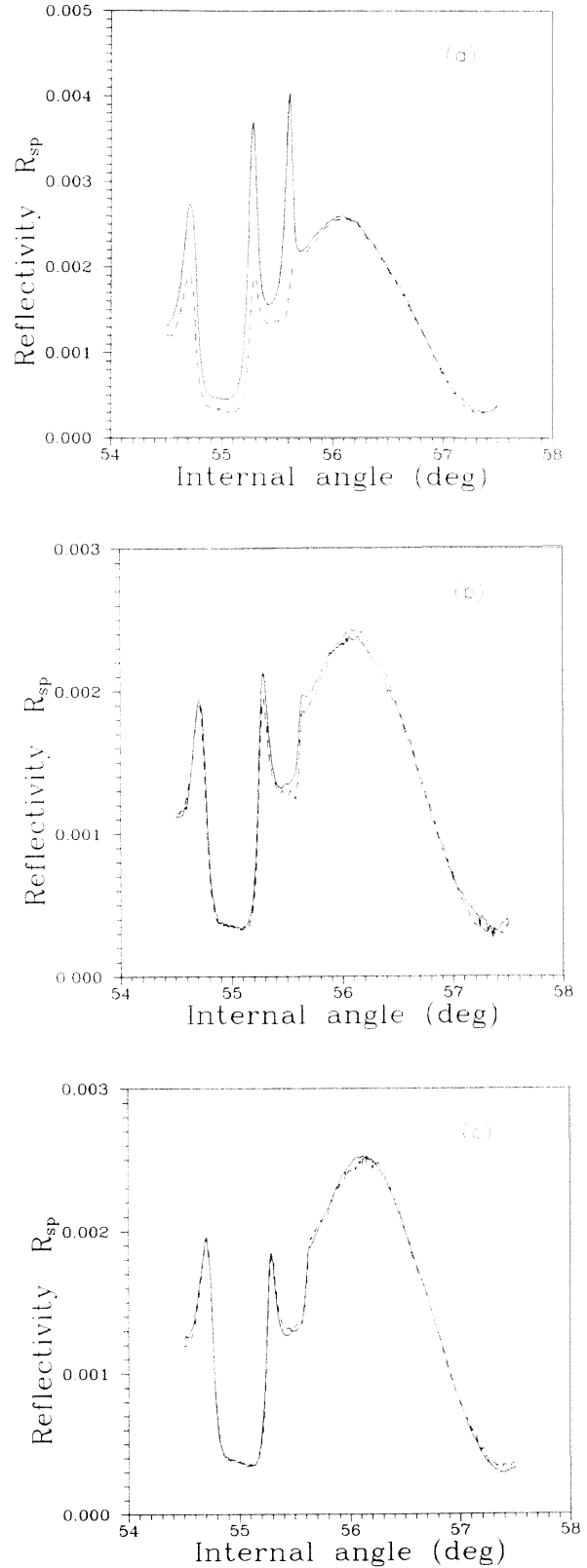


FIG. 4. Experimental reflectivity data under zero electric field conditions. The solid and dashed lines indicate the data obtained when the electric field is reduced to zero from +1500 and -1500 V, respectively, for temperatures of (a) $T_c - 0.2^\circ\text{C}$, (b) $T_c - 0.1^\circ\text{C}$, and (c) T_c .

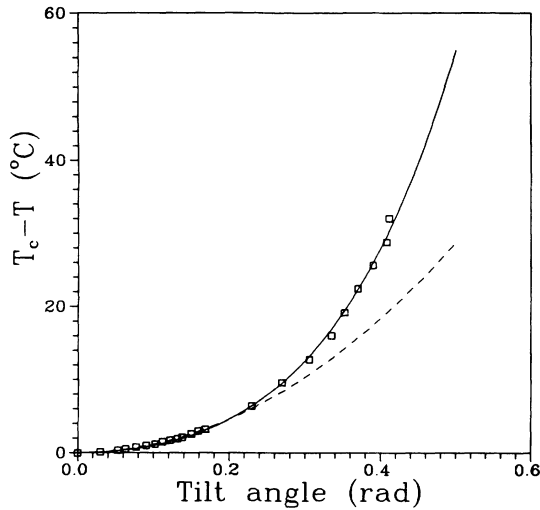


FIG. 5. Comparison of the experimental data with the extended mean-field theory. The solid line is the full extended mean-field theory fit, the dashed line is the simple mean-field theory fit to the data closest to T_c (see Fig. 6).

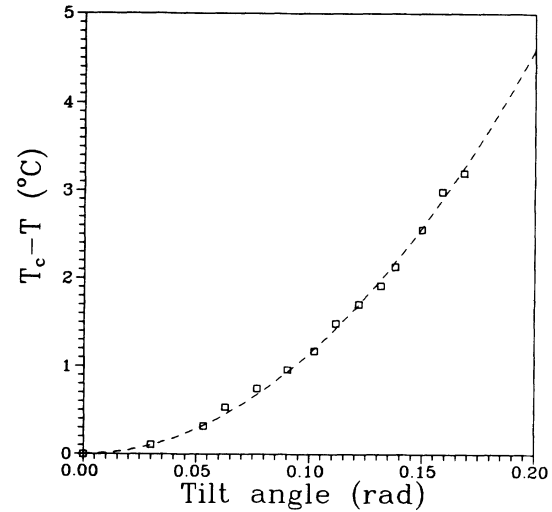


FIG. 6. Comparison of experimental data close to T_c with mean-field theory. The open squares are data and the dashed lines theory.

which is in full accord with the experimental data and gives $b = 0.144a$ and $c = 0.507a$.

In the extended mean-field theory there is a very important parameter [7] $t_0 = b^2/ac$ which characterizes the nature of the phase transition. If $t \ll t_0$ then $t \propto \theta^2$, which represents the critical behavior for the second-order mean-field transition. The fit to this dependence is shown in Fig. 6 (and also by the dashed line in Fig. 5), over the regime closest to T_c . Conversely, if $t \gg t_0$ then $t \propto \theta^4$, which is characteristic of tricritical behavior, while for $t \approx t_0$, then the exponent lies in the range 2–4 which is characteristic of heliumlike behavior. Hence if t_0 is small (10^{-3}) as in the previous measurements [17], then the crossover point is very close to T_c and the data will tend, misleadingly, to fit a simple power law and appear to confirm heliumlike behavior.

In the present experiment, $t_0 \approx 0.04$ and the crossover point is some 13.5°C below T_c . This is why in the region closer to T_c than this a θ^2 law pertains with our data never being far enough from T_c to give just a θ^4 dependence. Instead, we find a region in which the power relation has the form θ^N , where $2 < N < 4$. In reality the data fits the relation given in equation (1) over the whole of the temperature region of interest. This very clearly and unambiguously

establishes the extended mean-field behavior of the S_C^* and S_A transition in SCE13 through direct optical measurement of the director tilt angle.

In conclusion, by using the half-leaky guided mode technique, tilt angle studies have been carried out on a homeotropically aligned ferroelectric liquid crystal (SCE13) cell in the vicinity of the smectic- A –chiral-smectic- C transition. Because the alignment is realized by only applying an in-plane dc electric field to the cell constructed from two bare glass surfaces a uniform tilted monodomain is obtained and subsequently high resolution tilt angle measurements made. The relationship between the measured tilt angle and temperature for SCE13 is well described by an extended mean-field model with a large third-order term (in θ^2) in the free-energy expansion. For the material studied here, SCE13, the characterizing parameter t_0 is one order of magnitude higher than observed in previous results on other materials allowing an extended range of study of the mean-field-like behavior of the S_A – S_C^* transition for this liquid crystal.

ACKNOWLEDGMENT

The authors acknowledge the financial support of the Science and Engineering Research Council.

- [1] P. G. deGennes, *Mol. Cryst. Liq. Cryst.* **21**, 49 (1973).
- [2] M. Dalye and P. Keller, *Phys. Rev. Lett.* **35**, 1065 (1976).
- [3] D. Guillon and A. Skoulios, *J. Phys. (Paris)* **38**, 79 (1977).
- [4] S. Meiboom and R. C. Hewitt, *Phys. Rev. A* **15**, 2444 (1977).
- [5] C. R. Safinya, M. Kaplan, J. Als-Nielsen, R. J. Birgeneau, D. Davidot, J. D. Litster, D. L. Johnson, and N. E. Neubert, *Phys. Rev. B* **21**, 4149 (1980).
- [6] C. A. Shamtz and D. L. Johnson, *Phys. Rev. A* **17**, 1504

- (1978).
- [7] C. C. Huang and J. M. Viner, *Phys. Rev. A* **25**, 3385 (1982).
- [8] S. C. Lien, C. C. Huang, and J. W. Goodby, *Phys. Rev. A* **29**, 1371 (1984).
- [9] M. Meichle and C. W. Garland, *Phys. Rev. A* **27**, 2624 (1983).
- [10] J. Thoen and G. Seynhaeve, *Mol. Cryst. Liq. Cryst.* **127**, 229 (1985).

- [11] S. Dumrongrathana, G. Nounesis, and C. C. Huang, *Phys. Rev. A* **33**, 2181 (1986).
- [12] G. Nounesis, C. C. Huang, T. Pitchford, and E. Hobbie, *Phys. Rev. A* **35**, 1441 (1987).
- [13] C. C. Huang and S. Dumrongrathana, *Phys. Rev. A* **34**, 5020 (1986).
- [14] S. Dumrongrathana and C. C. Huang, *Phys. Rev. Lett.* **56**, 464 (1986).
- [15] H. Y. Liu, C. C. Huang, Ch. Bahr, and G. Heppke, *Phys. Rev. Lett.* **61**, 345 (1988).
- [16] Fuzi Yang and J. R. Sambles, *J. Opt. Soc. Am. B* **10**, 858 (1993).
- [17] S. C. Lien and C. C. Huang, *Phys. Rev. A* **30**, 624 (1984).

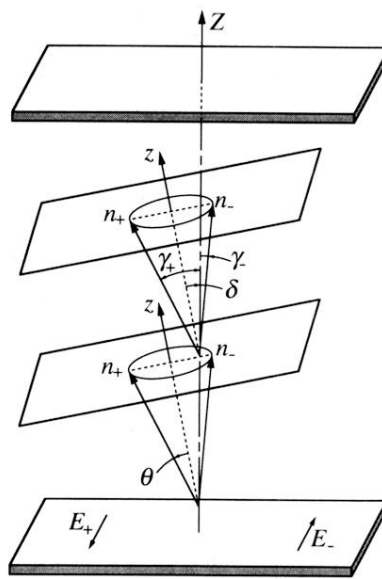


FIG. 3. The geometry associated with the unwinding of the helix with an applied dc electric field. θ is the cone angle of the liquid crystal and δ the angle between the normal to the cell wall and the normal of the layers. n_+, γ_1 and n_-, γ_2 are the unwound primary directors and measured tilt angle under positive E_+ and negative E_- dc fields, respectively.